

## Shot-based deghosting for variable sea surface and receiver depth

Vrolijk, Jan-Willem; Blacquièrè, Gerrit

**DOI**

[10.1190/segam2017-17742156.1](https://doi.org/10.1190/segam2017-17742156.1)

**Publication date**

2017

**Document Version**

Final published version

**Published in**

SEG Technical Program Expanded Abstracts 2017

**Citation (APA)**

Vrolijk, J.-W., & Blacquièrè, G. (2017). Shot-based deghosting for variable sea surface and receiver depth. In *SEG Technical Program Expanded Abstracts 2017: 24-29 September, Houston, USA* (pp. 4887-4892). (SEG Technical Program Expanded Abstracts 2017). <https://doi.org/10.1190/segam2017-17742156.1>

**Important note**

To cite this publication, please use the final published version (if applicable). Please check the document version above.

**Copyright**

Other than for strictly personal use, it is not permitted to download, forward or distribute the text or part of it, without the consent of the author(s) and/or copyright holder(s), unless the work is under an open content license such as Creative Commons.

**Takedown policy**

Please contact us and provide details if you believe this document breaches copyrights. We will remove access to the work immediately and investigate your claim.

## Shot-based deghosting for variable sea surface and receiver depth

Jan-Willem Vrolijk\* and Gerrit Blacquièrè, Delft University of Technology

### SUMMARY

Uncertainties in the water velocity, receiver location and sea surface state introduce noise and ringing after deghosting. Therefore, a shot-based deghosting method is discussed that includes a constraint to reduce this effect of inaccuracies in the ghost model. First, we show results for a flat cable with an accurate ghost model. After that, the deghosting method is applied to a shot with a slanted cable. Finally, an inaccurate ghost model is applied to a shot, that is modelled with a variable sea surface.

### INTRODUCTION

The source and receiver ghost effects in marine acquisition cause angle-dependent notches in the spectrum and severe attenuation of the low frequencies. In the case of standard seismic acquisition, deghosting is a challenging preprocessing step. Today, there is a renewed interest in ghost suppression because it removes the large sidelobes of the seismic wavelet and therefore, improves the image resolution significantly. In this revival, deghosting at the receiver side has received ample attention. Soubaras (2010) applies a joint deconvolution step to a direct and a mirror migration result. Wang and Peng (2012) introduce a bootstrap method based on the generation of mirror data with a 1D ray-tracing approximation. Amundsen et al. (2013) describe deghosting as a deterministic spatial deconvolution. Ferber et al. (2013) estimate the vertical particle-motion component from marine pressure data by convolving the result of a sparse deconvolution of the pressure ghost wavelet with the corresponding ghost wavelet of the particle motion. They continue with a conventional deghosting technique based on combining pressure data with particle velocity data. Beasley et al. (2013) and Robertsson et al. (2014) use the fact that the upcoming waves arrive earlier than the downgoing 'ghost' waves, leading to causal deghosting filters. Ferber and Beasley (2014) use this principle to shift the ghost events out of the time window.

In case of a perfectly calm sea, the sea surface reflection coefficient is known. However, the sea surface can be rough and the sea-surface reflection coefficient can be frequency-dependent (see Orji et al., 2013), which is not exactly known. Another uncertainty in the ghost model is the receiver depth measured during acquisition, the recorded depth is spatially interpolated and averaged over the recording time. A rough sea will result in a less accurate receiver location. In addition, temperature and salinity are temporally and spatially varying in the water column between receiver and the sea surface (Leroy et al., 2008), as a result of weather and tides. This affects the water velocity, thereby influencing the wave propagation. Deghosting is sensitive to errors in the ghost model, resulting from the uncertainties in the water velocity, receiver location and sea surface reflection. This can result in ringing in the deghosted

data. At the receiver side Rickett et al. (2014) developed an adaptive deghosting algorithm that takes into account small deviations in these parameters. King and Poole (2015) include a variable sea surface that is calculated from the data. Grion et al. (2015) described a method to maximize the kurtosis of the autocorrelation function, to determine which parameters give the best deghosting result. In order to make the deghosting result less sensitive to noise and errors in the ghost model we discuss a deghosting method based on a constraint in the time domain.

### DEGHOSTING: THE FORWARD MODEL

In marine acquisition, receivers are towed at some depth  $z_r$ , which is a spatially dependent variable, i.e.,  $z_r = z_r(x, y)$ . The water surface reflectivity at level  $z_0$  is very strong which means that two pressure wavefields are measured at a receiver: the first is directly travelling up, the second is going up, getting reflected at the water surface and then travelling down. The latter generates the so-called ghost response at the receiver side. We now formulate the forward model. The measured wavefield at the receiver side is the sum of the two wavefields mentioned: the direct one and the one reflected at the sea surface. Using the matrix notation (Berkhout, 1985), the process can be formulated as follows for each frequency component in the space domain:

$$\mathbf{D}(z_r) = \mathbf{D}_0(z_r)\mathbf{W}^+(z_r, z_0)\mathbf{R}^\cap(z_0, z_0)\mathbf{W}^-(z_0, z_r) + \mathbf{D}_0(z_r), \quad (1)$$

where operator  $\mathbf{D}_0$  describes the receiver properties at receiver depth  $z_r$ , the subscript 0 refers to the ghost-free situation, matrix  $\mathbf{R}^\cap$  describes the angle- and frequency-dependent surface reflectivity and matrices  $\mathbf{W}^-$  and  $\mathbf{W}^+$  describe up- and downward extrapolation, respectively. Equation 1 can be written as:

$$\mathbf{D}(z_r) = \mathbf{D}_0(z_r)\mathbf{G}^\cap(z_r, z_r), \quad (2)$$

where  $\mathbf{G}^\cap$  is the ghost operator at the receiver side given by

$$\mathbf{G}^\cap(z_r, z_r) = [\mathbf{W}^+(z_r, z_0)\mathbf{R}^\cap(z_0, z_0)\mathbf{W}^-(z_0, z_r) + \mathbf{I}(z_r, z_r)]. \quad (3)$$

The notch frequencies for arbitrary horizontal wavenumber and a situation without lateral variation in  $z_r$  become:

$$f_n(k_x) = \sqrt{\frac{nc}{2z_r} + k_x^2 c^2} \quad (4)$$

where  $n$  the order of the notch,  $c$  the water velocity and  $k_x$  the horizontal wavenumber. In extreme cases where the surface reflectivity  $\mathbf{R} = \mathbf{I}$ , the amplitude values at the notch locations become zero. In practise, the amplitudes are frequency and angle dependent (Orji et al., 2013).

Without lateral variation, extrapolation in the wavenumber frequency domain corresponds to a multiplication with:

$$\tilde{\mathbf{W}}^\pm(z_r, z_0) = e^{\pm jk_x \Delta z}, \quad (5)$$

## Shot-based deghosting

where  $k_z = \sqrt{k^2 - k_x^2}$ ,  $k = 2\pi f/c$ , with  $f$  being frequency and  $\Delta z = z_r - z_0$ . The tilde symbol  $\tilde{\cdot}$  indicates the wavenumber-frequency domain. Extrapolation in the space-frequency domain therefore corresponds to a convolution, which can be numerically implemented as a matrix multiplication, the rows, corresponding to the receiver location of this matrix containing the inverse Fourier transform of  $\tilde{\mathbf{W}}^\pm$ . The water velocity or depth  $\Delta z$  may be different for each receiver, which means that lateral changes can be accommodated for. The matrices obtained in this way are the  $\mathbf{W}^\pm$  in the space-frequency domain as they appear in the equations. In Berkhout (1985), Blacquière et al. (1989) and Thorbecke et al. (2004) the propagation matrix is discussed extensively.

The model for a shot gather including the receiver ghost is:

$$\tilde{P}(z_r; z_s) = \mathbf{D}_0(z_r) \mathbf{G}^\cap(z_r, z_r) \mathbf{X}^\cup(z_r, z_0) \tilde{S}_0(z_0), \quad (6)$$

where the source is located at  $z_0$ ,  $\tilde{S}_0$  is the source pressure field,  $\mathbf{X}^\cup$  is the Earth transfer function and  $\tilde{P}$  is a monochromatic shot record. Finally the model can be easily extended to include the ghost response related to sources at level  $z_s(x, y)$  as well:

$$\tilde{P}(z_r; z_s) = \mathbf{D}_0(z_r) \mathbf{G}^\cap(z_r, z_r) \mathbf{X}^\cup(z_r, z_s) \mathbf{G}^\cap(z_s, z_s) \tilde{S}_0(z_s), \quad (7)$$

where  $\mathbf{G}^\cap$  at the right of  $\mathbf{X}^\cup$  is the ghost operator at the source side.

As for the inverse ghost operator, it becomes unstable in the case of  $\mathbf{R} = \mathbf{I}$  due to zeros in the denominator (see equation 3). In addition, near the notch frequencies, the signal-to-noise ratio (SNR) is usually low, which prevents a successful spectral division. This means that the noise inside the notch areas will be amplified by applying the inverse operator  $[\mathbf{G}^\cap]^{-1}$  and this has a detrimental effect on the overall SNR of the data. In the following section a deghosting method that is able to control noise is discussed.

### DEGHOSTING: AN INVERSE PROBLEM

The action of receiver deghosting means that a shot gather with receiver ghost (equation 7) is turned into a shot gather without receiver ghost:

$$\tilde{P}_0(z_r; z_s) = \mathbf{D}_0(z_r) \mathbf{X}^\cup(z_r, z_s) \mathbf{G}^\cap(z_s, z_s) \tilde{S}_0(z_s). \quad (8)$$

Comparing equations 7 and 8 makes clear that receiver deghosting means:

$$\tilde{P}_0(z_r) = \mathbf{D}_0(z_r) [\mathbf{G}^\cap(z_r, z_r)]^{-1} [\mathbf{D}_0(z_r)]^{-1} \tilde{P}(z_r), \quad (9)$$

with  $\tilde{P}(z_r; z_s)$  including the source ghost effect. Note that a deconvolution for the receiver properties has been carried out in equation 9, this benefit can be preserved by defining the receiver deghosting process as follows:

$$\tilde{P}_0(z_r) = \hat{\mathbf{I}}(z_r) [\mathbf{G}^\cap(z_r, z_r)]^{-1} [\mathbf{D}_0(z_r)]^{-1} \tilde{P}(z_r), \quad (10)$$

where matrix  $\hat{\mathbf{I}}(z_r)$  indicates an ideal spatial sampling of receivers.

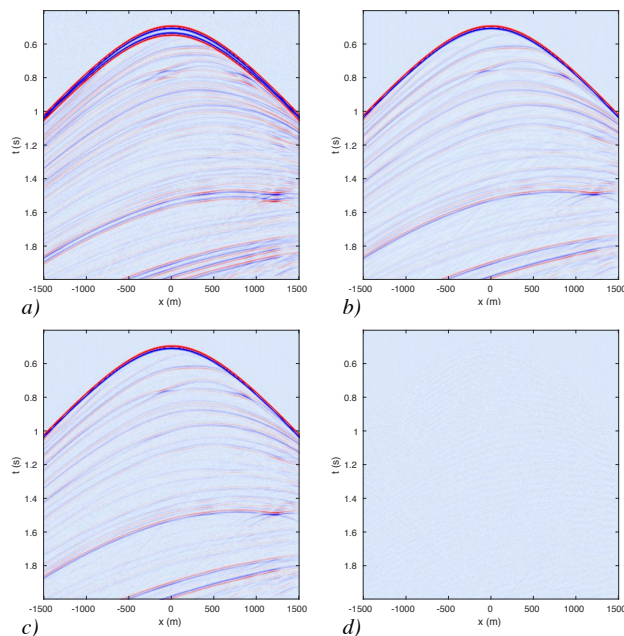


Figure 1: Results for a synthetic shot record with receivers at  $z_r = 20$  m. a) Input shot record including the ghost effect (SNR=20 dB). b) Modelled ghost-free shot record. c) Shot record after closed-loop deghosting. d) Residual between Figures b) and c).

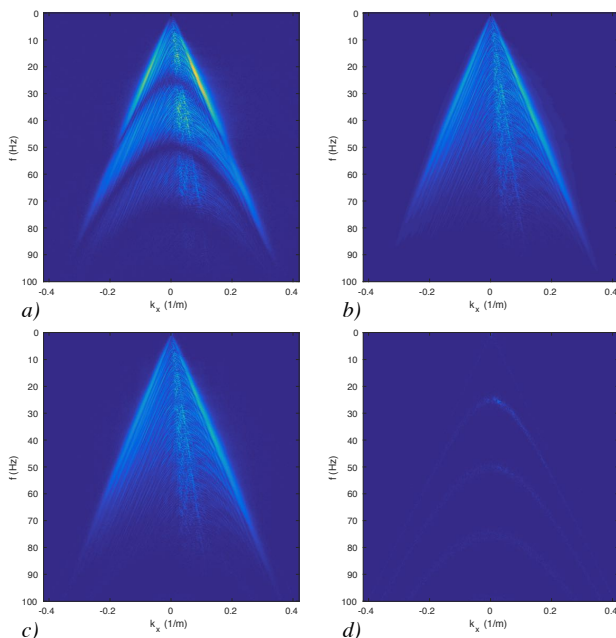


Figure 2: Results for a synthetic shot record with receivers at  $z_r = 20$  m in the space frequency domain. a) Input shot record including the ghost effect (SNR=20 dB). b) Modelled ghost-free shot record. c) Shot record after closed-loop deghosting. d) Residual between Figures b) and c).

## Shot-based deghosting

### CLOSED-LOOP DEGHOSTING

A least-squares iterative inversion is used to determine  $\vec{P}_0$  without explicitly calculating  $[\mathbf{G}^\cap(z_r, z_r)]^{-1}$  and  $\mathbf{D}_0(z_r)^{-1}$ . In Özdemir et al. (2008) a similar inversion is used to apply deghosting to over/under streamers. The output consists of the deghosted response corresponding to the real receivers at  $z_r$ . The method is based on minimizing the following objective function:

$$J = \sum_{\omega} \|\vec{P}(z_r; z_s) - \mathbf{D}_0(z_r)\mathbf{G}^\cap(z_r, z_r)\vec{P}_0(z_r; z_s)\|^2 + \lambda \|\vec{p}_0(z_r; z_s)\|_S, \quad (11)$$

where  $\|\cdot\|_S$  is a sparsity-promoting norm,  $\lambda$  is a user defined constant to control this norm and  $\vec{p}_0$  is the ghost free shot gather in the time domain. The L1 norm is added as a sparsity-promoting norm to the objective function (see equation 11). A conjugate gradient scheme that minimizes equation 11 is used to iteratively converge to  $\vec{P}_0$ . We will refer to this method as 'closed-loop deghosting'. In Rickett et al. (2014) a similar objective function is described in the Radon domain including the ghost delay times that are constrained by the L1 norm.

A shot record with receiver ghost effect is modeled from the Marmousi model using an 2D acoustic finite-difference scheme (see Figures 1a and 2a). The spatial detector sampling is 5 m, the time sampling is 4 ms and the detector depth is 20 m. Noise was added, the SNR being 20 dB. The results after closed-loop deghosting for Figures 1a and 2a are shown in Figures 1c and 2c. The signal seem to be recovered accurately, there are only ghost-free events without ringing. The difference (Figures 1b and 2b) between the modelled ghost-free shot record (Figures 1b and 2b) and the shot gather after closed-loop deghosting (Figures 1c and 2c) show that only in the notch area there is a small error. Furthermore the noise level seems to be similar to the input data. In Vrolijk and Blacquière (2017) an approach to quantify signal reconstruction and noise is discussed.

### VARIABLE RECEIVER DEPTH

The slanted streamer introduced in early 1980s (Ray, 1982) has several benefits. They often provide a higher resolution image and the signal-to-noise ratio is better, especially for the lower frequencies. The improved signal-to-noise ratio is the consequence of a deeper position of the cable for larger offsets. The variable depth of the streamer results in ghost notch diversity. Therefore the  $\mathbf{W}^\pm$  at the receiver side (see equation 3) must take into account variable depths and therefore applied in the space-frequency domain. If the slanted cable geometry varies between shot records, e.g. due to feathering,  $\mathbf{W}$  will become shot dependent. An estimate of the depth of each receiver is measured during acquisition.

Closed-loop deghosting is applied to a broadband (3-150 Hz) shot record from offshore Australia, provided by CGG. Closed-loop deghosting is applied with the  $\mathbf{G}$  operator now describing the effect of a slanted cable with a depth increasing from 8 to 57.5 m. The receiver sampling is 12.5 m and time sampling is 2 ms. In Figure 3a and 3c the input data for closed-loop deghosting is shown, respectively in the shot and zoomed shot domain. A bandpass filter and  $fk$ -filter is applied to the shot for display

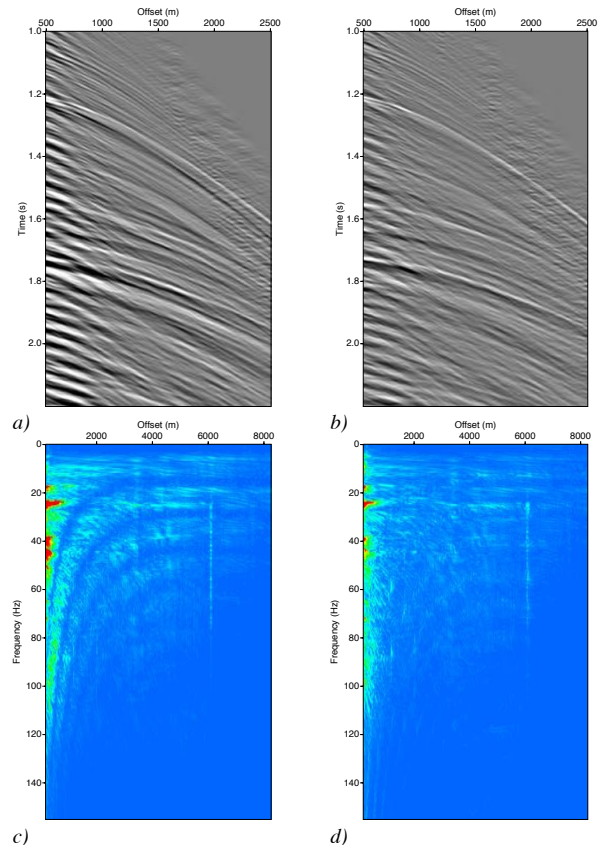


Figure 3: Receiver deghosting result for a shot record with a slanted cable, a) zoomed input shot record, b) zoomed shot record after closed-loop deghosting, c) input shot-record in space-frequency domain, d) shot-record after closed-loop deghosting in space-frequency domain.

purpose. Figures 3b and 3d are the ghost-free primaries, thus the outcome of closed-loop deghosting. The deghosting for the slanted cable is quite accurate: the events around 1.25 s. and 1.75 s, that clearly display the slanted-cable ghost effect (Figures 3a and 3c), have become ghost-free after closed-loop deghosting (Figures 3b and 3d). In Figure 3d the notch frequencies that are offset-dependent due to the slant of the cable (see Figure 3c) are filled in after deghosting, the noise inside notch area is amplified a bit in areas where signals-to-noise ratio is low.

### VARIABLE SEA SURFACE

Wind can create waves that will result in a variable sea surface and this changes the relative receiver depth with respect to the sea surface. A variable sea surface is modelled and its ghost effect, corresponding to a varying depth around 20 m, is modeled with a standard Kirchoff method (Laws and Kragh, 2002; Pierson and Moskowitz, 1964). This response is convolved with a ghost-free shot-record of the marmousi model and noise is added to the data (Figures 4a and 5a). The ghost operator  $\mathbf{G}^\cap$  used during the closed-loop deghosting has a fixed depth of 20m. In order to suppress artefacts that will be in-

## Shot-based deghosting

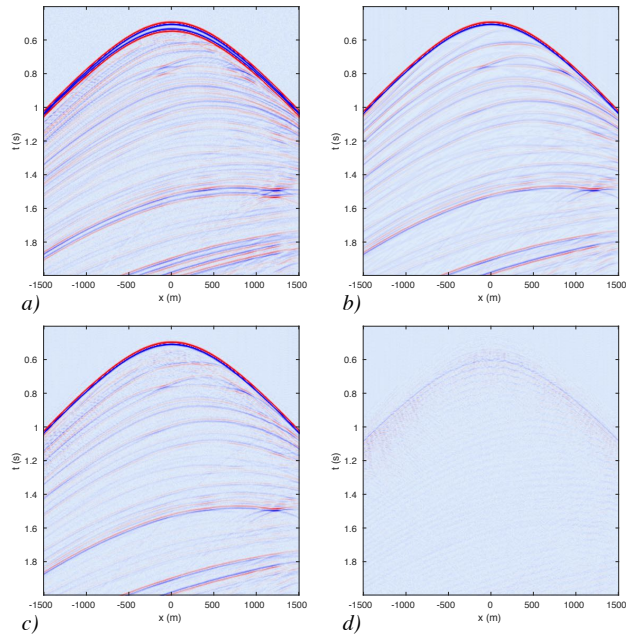


Figure 4: Results for a shot record with receivers varying around  $z_r = 20$  m. a) Input shot including the ghost effect (SNR=20 dB). b) Modelled ghost-free shot record. c) Shot record after closed-loop deghosting. d) Residual between Figures b) and c).

roduced by an inaccurate ghost operator more weight is put on the sparseness constraint with respect to an accurate ghost operator. After closed-loop deghosting (Figures 4b and 5b) the ghost-free events are estimated and the notch areas are recovered. However, in the wavenumber-frequency domain of the shot gather after closed-loop deghosting (Figure 4b) there is a small imprint of the first-order notch. Near the first arrival, ringing events and noise leaked into the shot record after deghosting. In the residual (Figure 4d) between the modelled ghost-free shot record (Figure 5a) and shot gather after closed-loop deghosting (Figure 5c) this effect is evident. This means there is a limit to the accuracy of closed-loop deghosting using an inaccurate ghost model. For a more accurate result, a more accurate ghost operator must be estimated prior to deghosting or the ghost operator needs to be refined during the iterative deghosting method.

## CONCLUSION

In this paper a deghosting method is discussed that is able to handle inaccuracies in the ghost model. In addition, variable depths of receivers can be included in the propagation matrices, if known a-priori. Accurate results are obtained for a modelled shot record with a fixed cable depth. The closed-loop method is successfully applied to a shot record from a field data set with a slanted cable. It is shown that after closed-loop deghosting, in the presence of a variable sea surface and an inaccurate ghost operator, noise is suppressed. However, there is still noise and ringing present in the deghosted shot

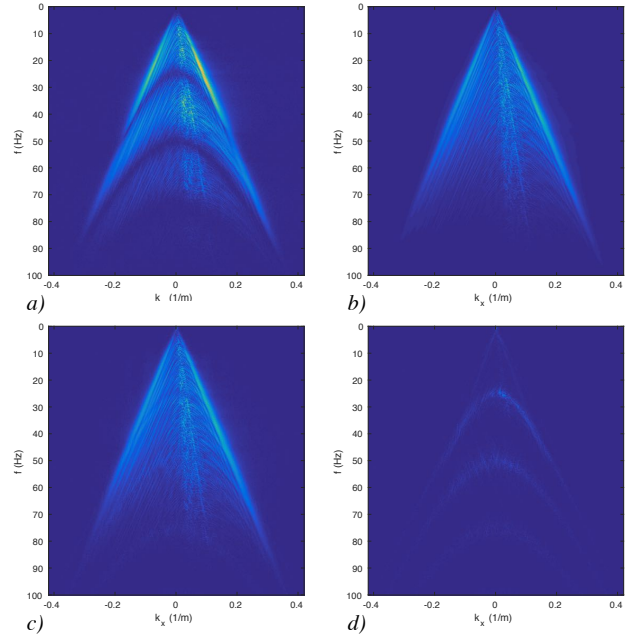


Figure 5: Results for a shot record with receivers varying around  $z_r = 20$  m in the space-frequency domain. a) Input shot record including the ghost effect (SNR=20 dB). b) Modelled ghost-free shot c) Shot record after closed-loop deghosting. d) Residual between Figures c) and d).

gather. Therefore, the next step is to make the deghosting method adaptive to inaccuracies in the ghost operator that are inherent to errors in the sea surface reflection, water velocity and depth of receivers. This can be done by estimating more accurate matrices  $\mathbf{W}^{\pm}$  and  $\mathbf{R}$  from the data prior to deghosting or by refining the ghost operator during the inversion.

## ACKNOWLEDGMENTS

We would like to thank CGG for providing the field data set and we acknowledge the sponsors of the Delphi consortium for the stimulating discussions during the Delphi meetings and their continuing financial support support.

## EDITED REFERENCES

Note: This reference list is a copyedited version of the reference list submitted by the author. Reference lists for the 2017 SEG Technical Program Expanded Abstracts have been copyedited so that references provided with the online metadata for each paper will achieve a high degree of linking to cited sources that appear on the Web.

## REFERENCES

- Amundsen, L., H. Zhou, A. Reitan, and A. B. Weglein, 2013, On seismic deghosting by spatial deconvolution: *Geophysics*, **78**, no. 6, V267–V271, <https://doi.org/10.1190/geo2013-0198.1>.
- Beasley, C. J., R. Coates, Y. Ji, and J. Perdomo, 2013, Wave equation receiver deghosting: a provocative example: 83rd Annual International Meeting, SEG, Expanded Abstracts, **32**, 4226–4230, <https://doi.org/10.1190/segam2013-0693.1>.
- Berkhout, A. J., 1985, *Seismic migration, volume a: Theoretical aspects*: (3rd ed.): Elsevier.
- Blacquiere, G., H. W. J. Debeye, C. P. A. Wapenaar, and A. J. Berkhout, 1989, 3-D table-driven migration: *Geophysical Prospecting*, **37**, 925–958, <https://doi.org/10.1111/j.1365-2478.1989.tb02241.x>.
- Ferber, R., and C. J. Beasley, 2014, Simulating ultra-deep-tow marine seismic data for receiver deghosting: 76th Annual International Conference and Exhibition, EAGE, Extended Abstracts, <https://doi.org/10.3997/2214-4609.20141452>.
- Ferber, R., P. Caprioli, and L. West, 2013, L1 pseudo-vz estimation and deghosting of single-component marine towed streamer data: *Geophysics*, **78**, no. 2, WA21–WA26, <https://doi.org/10.1190/geo2012-0293.1>.
- Grion, S., R. Telling, and J. Barnes, 2015, De-ghosting by kurtosis maximisation in practice: 85th Annual International Meeting, SEG, Expanded Abstracts, 4605–4609, <https://doi.org/10.1190/segam2015-5902239.1>.
- King, S., and G. Poole, 2015, Hydrophone-only receiver deghosting using a variable sea surface datum: 85th Annual International Meeting, SEG, Expanded Abstracts, 4610–4614, <https://doi.org/10.1190/segam2015-5891123.1>.
- Laws, R., and E. Kragh, 2002, Rough seas and time-lapse seismic: *Geophysical Prospecting*, **50**, 195–208, <https://doi.org/10.1046/j.1365-2478.2002.00311.x>.
- Leroy, C. C., S. P. Robinson, and M. J. Goldsmith, 2008, A new equation for the accurate calculation of sound speed in all oceans: *Journal of Acoustical Society of America*, **124**, 2774–2782, <https://doi.org/10.1121/1.2988296>.
- Orji, O. C., W. Sollner, and L. J. Gelius, 2013, Sea surface reflection coefficient estimation: 83rd Annual International Meeting, SEG, Expanded Abstracts, 51–55, <https://doi.org/10.1190/segam2013-0944.1>.
- Ozdemir, A. K., P. Caprioli, A. Ozbek, E. Kragh, and J. A. Robertsson, 2008, Optimized deghosting of over/under towed-streamer data in the presence of noise: *The Leading Edge*, **27**, 190–192, <https://doi.org/10.1190/1.2840366>.
- Pierson, W. J., and L. Moskowitz, 1964, A proposed spectral form for fully developed wind seas based on the similarity theory of S. A. Kitaigorodskii: *Journal of Geophysical Research*, **69**, 5181–5190, <https://doi.org/10.1029/JZ069i024p05181>.
- Ray, C., 1982, High resolution marine stratigraphic system: U. S. Patent 4353121 A.
- Rickett, J., D.-J. V. Manen, P. Loganathan, and N. Seymour, 2014, Slanted-streamer data-adaptive deghosting with local plane waves: 76th Annual International Conference and Exhibition, EAGE, Extended Abstracts, 4221–4225, <https://doi.org/10.3997/2214-4609.20141453>.
- Robertsson, J. O. A., L. Amundsen, and O. Pedersen, 2014, Deghosting of arbitrarily depth-varying marine hydrophone streamer data by time-space domain modelling: 84th Annual International Meeting, SEG, Expanded Abstracts, 4248–4252, <https://doi.org/10.1190/segam2014-0221.1>.

- Soubaras, R., 2010, Deghosting by joint deconvolution of amigration and a mirror migration: 80th Annual International Meeting, SEG, Expanded Abstracts, **29**, 3406–3410, <https://doi.org/10.1190/1.3513556>.
- Thorbecke, J. W., C. P. A. Wapenaar, and G. Swinnen, 2004, Design of one-way wavefield extrapolation operators, using smooth functions in WLSQ optimization: Geophysics, **69**, 1037–1045, <https://doi.org/10.1190/1.1778246>.
- Vrolijk, J. W., and G. Blacqui`ere, 2017, Deghosting and its effect on noise: 79th Annual International Conference and Exhibition, EAGE, Extended Abstracts.
- Wang, P., and C. Peng, 2012, Premigration deghosting for marine towed streamer data using a bootstrap approach: 82nd Annual International Meeting, SEG, Expanded Abstracts, **31**, 1–5, <https://doi.org/10.1190/segam2012-1146.1>.